D. Invernizzi, M. Lovera
A Projection-Based Controller for Fast Spacecraft Detumbling Using Magnetic Actuation
Automatica, Vol. 113, 2020, 108779 (10 pages)
doi:10.1016/j.automatica.2019.108779

A projection-based controller for fast spacecraft detumbling using magnetic actuation

Davide Invernizzi [a], Marco Lovera [a]

[a] *Politecnico di Milano, Department of Aerospace Science and Technology, Via La Masa 34, 20156, Milano*

Abstract

Magnetic control has been used for decades for spacecraft detumbling, *i.e.*, to bring a spacecraft to a final condition with a sufficiently small angular momentum after separation from the launcher. This task is typically achieved by controllers based on the so-called *b-dot* principle, which stands out thanks to its simplicity, reliability and ease of on-board implementation. In this paper, we first review existing control methods and study their convergence properties with tools borrowed from general averaging theory, which allows addressing in an accurate manner the time-varying nature of magnetic actuation. Then, some effort is devoted to showing the performance limitations of existing controllers for which increasing the gain too much deteriorates the convergence rate. To overcome this issue, a novel projection-based control law with a state-dependent time-varying gain is presented. By means of Lyapunov arguments for non-autonomous systems, we prove that the proposed controller guarantees that the spacecraft angular momentum converges exponentially fast to zero for all initial conditions, robustly with respect to sufficiently small uncertainties in the inertia matrix, and that the closed-loop solutions are globally uniformly ultimately bounded in the presence of exogenous disturbances. Several numerical simulations have been carried out by referring to realistic detumbling scenarios to show the performance improvement with respect to existing controllers.

1 Introduction

Magnetic coils have been used since the beginning of the space age as a simple and efficient torque generation mechanism for attitude and momentum control of Low Earth Orbit (LEO) satellites [22]. Their operation is based on the interaction between the magnetic dipole generated by the coils and the magnetic field of the Earth and therefore provides a simple solution to the problem of generating torques on board a spacecraft. More precisely, magnetic torquers can be used either as main actuators for attitude control in momentum biased or gravity gradient architectures or as secondary actuators for momentum management tasks in zero momentum reaction wheels-based configurations.

The main issue associated with magnetic coils is the fact that magnetic torques are constrained to lie in the plane orthogonal to the local magnetic field, so that the angular dynamics of a magnetically actuated spacecraft is completely controllable only in the time-varying sense (due to the variability of the geomagnetic field). This leads to a number of difficulties in the design of the attitude control law, which have been studied extensively in the last few years. In particular, as far as the design of nominal attitude control laws is concerned the recent work has focused on the application of optimal and robust periodic control theory to a number of attitude control system (ACS) configurations, namely gravity gradient spacecraft [28,21], momentum biased spacecraft [20,18,13,22,7], or satellites exploiting passive aerodynamic properties [29]. The global formulation of the problem has also been studied extensively, both for Earth pointing (see, *e.g.*, [27,5,2,25]) and inertially pointing (see [15,16,11]) spacecraft.

Detumbling consists in bringing the spacecraft from an initial condition possibly characterized by a large angular momentum, to a final one which, while remaining essentially arbitrary in terms of direction of the angular rate vector, is compatible with the operation of subsequent ACS modes. Limited attention, with the partial exception of the recent papers [10,1,6], has been devoted to studying the detumbling problem in a systematic manner, which is the first task the ACS must perform after separation of the spacecraft from the launcher. Detumbling must be performed by the spacecraft in a fully autonomous way. Therefore, in order to minimize the risk of failure in the course of this operation, tight requirements on the reliability of the involved actuators and sensors and on the simplicity of the adopted control law are usually driving the design of the detumbling mode. It is worth underling that magnetic torquers are

Email addresses: davide.invernizzi@polimi.it (Davide Invernizzi), marco.lovera@polimi.it (Marco Lovera).

extremely reliable, as they do not involve moving parts and are therefore less sensitive to the large vibratory loads during launch than, *e.g.*, inertial actuators. Similarly, magnetometers are reliable, relatively inexpensive equipment, which can be easily redunded if necessary. The idea enabling detumbling by using only magnetic actuators and sensors is the *b-dot* algorithm (in all its variants developed and flown through the years [23,8])), which is still currently the most used method considered for spacecraft detumbling [9,30]. More recent approaches are projection-based control designs which combine magnetometer and state feedback measurements to provide the desired dissipation of the spacecraft kinetic energy. Nonlinear model predictive control techniques have also been considered in numerical studies [29,1] but their on-board implementation is still hindered by the complexity of such control designs for a mission-critical task like detumbling.

Following the approach of the preliminary paper [14], we rely on general averaging theory [12] to show that for a sufficiently small gain, existing projection-based controllers [10,17,24] can achieve an exponential convergence rate without relying on the periodicity assumption for the time-variability of the geomagnetic field [27]. This small gain analysis goes beyond the asymptotic result of [10] and is actually not limiting of the achievable performance of such controllers: we formally prove that using too large a damping gain results in a slow detumbling. Such misbehavior has been thoroughly studied in [10], in which a quasi-optimal gain value, proportional to the orbital rate, has been proposed to guarantee a satisfactory level of performance. To overcome this limitation, we propose a projection-based momentum controller combined with a time-varying state-dependent gain which allows handling in an efficient manner the instantaneous underactuation of magnetic control. By employing Lyapunov arguments for non-autonomous systems, we prove that our controller guarantees global exponential convergence in ideal conditions and robustness with respect to uncertainty in the knowledge of the spacecraft inertia matrix. Furthermore, by means of Input-to-State Stability (ISS) arguments we show that the closed-loop solutions are globally uniformly ultimately bounded in the presence of exogenous torques. The performance improvement with respect to state-of-the art approaches (settling-time reduced up to about 30%) is shown by means Monte Carlo simulations. Finally, note that the proposed approach can be as well exploited to improve momentum management tasks with magnetic control in reaction wheel-based configurations.

The paper is organized as follows. In Section 2 the mathematical model of magnetically actuated spacecraft for detumbling is recalled while the corresponding control problem is formalized in Section 3. Existing controllers are presented and discussed in Section 4. Section 5 is devoted to analyzing the large gain/slow convergence problem affecting existing designs. The controller proposed in this work is presented in details in Section 6 and finally, simulation results are provided in Section 7.

Notation $\mathbb{R}\,(\mathbb{R}_{>0}, \mathbb{R}_{\geq 0})$ denotes the set of (positive, nonnegative) real numbers, $\mathbb{Z}$ denotes the set of integers, $\mathbb{R}^n$ denotes the n-dimensional Euclidean space and $\mathbb{R}^{m\times n}$ the set of $m \times n$ real matrices. For $x \in \mathbb{R}^n$, $\|x\|$ is the Euclidean norm. For $A \in \mathbb{R}^{n\times n}$, $\|A\|$ is the ℓ_2-norm (spectral norm), *i.e.*, the square root of the largest eigenvalue of $A^\top A$. The minimum and maximum eigenvalues of $A \in \mathbb{R}^{n\times n}$ are denoted as $\lambda_m(A)$ and $\lambda_M(A)$, respectively. The unit vectors corresponding to the canonical basis in $\mathbb{R}^n$ are $e_i := [0, \ldots, 0, 1, 0, \ldots, 0]^\top$ for $i = 1, \ldots, n$ (vector with a 1 in the *i-th* coordinate and 0's elsewhere). The identity matrix in $\mathbb{R}^{n\times n}$ is denoted as $I_n := [e_1 \cdots e_i \cdots e_n]$. The third-order Special Orthogonal group is denoted as $\mathrm{SO}(3) := \{A \in \mathbb{R}^{3\times 3} : A^\top A = I_3, \det(A) = 1\}$ and its Lie algebra as $\mathfrak{so}\,(3) := \{W \in \mathbb{R}^{3\times 3} : W = -W^\top\}$, namely the space of third order skew-symmetric matrices. Given $\omega \in \mathbb{R}^3$, the *hat* map $S : \mathbb{R}^3 \to \mathfrak{so}(3)$ is an isomorphism between $\mathbb{R}^3$ and $\mathfrak{so}(3)$ such that $S(y)\omega = \omega \times y\ \forall y \in \mathbb{R}^3$, where $\times$ is the cross product operator. The set of piecewise-continuous and bounded functions is denoted as $\mathcal{L}_\infty$. We exploit standard nomenclature for comparison functions [12], in particular, a continuous function $\alpha : [0, a) \to \mathbb{R}_{\geq 0}$ for $a \in \mathbb{R}_{\geq 0}$ is of class$-\mathcal{K}$ if it is strictly increasing and $\alpha(0) = 0$. It is of class $\mathcal{K}_\infty$ if $a = \infty$ and $\alpha(s) \to \infty$ as $s \to \infty$. A continuous function $\beta : [0, a) \times \mathbb{R}_{\geq 0} \to \mathbb{R}_{\geq 0}$ belongs to class$-\mathcal{KL}$ if, for each fixed s, the mapping $\beta(r, s)$ belongs to class-$\mathcal{K}$ relative to r and, for each fixed r, it is nonincreasing relative to s and $\lim_{s\to\infty} \beta(r, s) = 0$.

2 Magnetically controlled spacecraft model

The model of a rigid spacecraft with magnetic actuation can be described in various reference frames [26]. For the purpose of the present analysis, we consider an Earth Centered Inertial frame (ECI) and a body frame with principal axes of inertia. In this setting, the configuration of a rigid body is uniquely and globally described by the rotation matrix $A := [\,j_1\ j_2\ j_3\,]^\top \in \mathrm{SO}(3)$, where j_1, j_2, j_3 are the unit vectors of the body frame resolved in the ECI frame. The attitude kinematics, which governs the time evolution of the body-fixed axes with respect to the ECI ones, is given by

$$\dot{A} = S(\omega)A, \tag{1}$$

where $\omega \in \mathbb{R}^3$ is the *body* angular velocity. The attitude dynamics of a magnetically actuated and rigid spacecraft can be expressed in body coordinates by Euler's equation [26]:

$$J\dot{\omega} = S(\omega)J\omega + \tau_m(t), \quad t \geq 0, \tag{2}$$

where $J = J^\top \in \mathbb{R}^{3\times 3}$ is the *body* inertia matrix and $\tau_m(t) \in \mathbb{R}^3$ is the torque delivered by the magnetic coils. As common in the literature on spacecraft detumbling [19,10,14], no exogenous torque is included in the model (2) since the conditions typical of such mode are dominated by inertial and control torques: the disturbance terms affect only the steady state behavior. Magnetic coils, which are assumed to be aligned with the spacecraft principal axes of inertia, generate a torque according to the cross product law

$$\tau_m(t) = m \times \tilde{b}(t) = S(\tilde{b}(t))m, \quad (3)$$

where $m \in \mathbb{R}^3$ is the vector of magnetic dipoles for the three coils (the physical control input) and $\tilde{b}(t) \in \mathbb{R}^3$ is the vector formed with the components of the Earth magnetic field in the body-fixed frame, which is measured on board. Note that $\tilde{b}(t)$ can be expressed in terms of the rotation matrix A and of the magnetic field vector expressed in the inertial coordinates, denoted as $\tilde{b}_0(t)$, as follows:

$$\tilde{b}(t) = A(t)\tilde{b}_0(t). \quad (4)$$

The orthogonality of A implies that $\|\tilde{b}(t)\| = \|\tilde{b}_0(t)\|$. When assuming that the spacecraft orbital motion is known, the values of $\tilde{b}_0(t)$ can be computed from a model of the geomagnetic field, such as the International Geomagnetic Reference Field (IGRF) (see [26]). For convenience, we denote $b(t)$ and $b_0(t)$ the unit vectors associated with $\tilde{b}(t)$ and $\tilde{b}_0(t)$, respectively, *i.e.*:

$$b(t) := \frac{\tilde{b}(t)}{\|\tilde{b}(t)\|} \qquad b_0(t) = \frac{\tilde{b}_0(t)}{\|\tilde{b}_0(t)\|}. \quad (5)$$

3 Magnetic detumbling: control problem formulation and related challenges

This section is devoted to presenting the detumbling problem for a magnetically controlled spacecraft and to showing the main challenges of the control design. Broadly speaking, the objective of detumbling is to bring the angular velocity of a spacecraft from arbitrary initial values to, ideally, zero. As mentioned in the Introduction, this operation is mission-critical and needs to be done quickly. The related stabilization problem is formalized as follows.

Problem 1 *Given the dynamical model of a magnetically controlled spacecraft described by equations* (1)-(3)*, find a control law for input $m \in \mathbb{R}^3$ such that the closed-loop trajectories converge to $\omega = 0$ as $t \to \infty$ from all initial conditions $(A(t_0), \omega(t_0)) \in \mathrm{SO}(3) \times \mathbb{R}^3$, $t_0 \geq 0$, when assuming that the body components of the geomagnetic field and of the angular velocity are available for feedback.*

Facing Problem 1 is challenging because the dynamical model (1)-(3) is time-varying, nonlinear and underactuated. The underactuation is due to the fact that the time-varying matrix $S(\tilde{b}(t))$ is skew-symmetric and therefore structurally singular. In particular, it is easy to see that $\mathrm{rank}(S(\tilde{b}(t))) = 2$ (since $\|\tilde{b}_0(t)\| \neq 0$ along all orbits of practical interest for magnetic control) and that the kernel of $S(\tilde{b}(t))$ is given by the vector $\tilde{b}(t)$ itself, *i.e.*, at each time instant it is *not* possible to apply a control torque along the direction of $\tilde{b}(t)$ [1].

4 Overview of existing methods for magnetic detumbling

In this section we will review the most common strategies which have been proposed in the literature to address the spacecraft detumbling problem by means of magnetic actuation alone. In our review we start by presenting control design based on the celebrated *b-dot* principle, in all its variants developed and flown through the years [8,14], which is undoubtedly the most adopted approach to spacecraft detumbling. The outstanding feature of the *b-dot* design is that it solely needs measurements coming from a magnetometer. More recent approaches to tackle the detumbling problem are projection-based state feedback methods (short, PBSF)) [17,10,24] and control designs based on nonlinear model predictive control. As we mentioned in the Introduction, model predictive techniques have been considered only in simulations [29,1] and their on-board implementation is hindered by the too high complexity for the stringent requirements, in terms of reliability and simplicity of the control law, of the detumbling phase. Instead, PBSF controllers are simple and computationally efficient and achieve zero steady state error in ideal conditions (no disturbance torques), a result which cannot be obtained by *b-dot*-based designs [2].

4.1 The b-dot principle

Magnetic field measurements can provide attitude information (in the form of a vector measurement), but cannot provide direct angular velocity information, which would be useful to produce a dissipative torque by means of (3). The magnetometer output, however, becomes relevant if one considers the time derivative of the measured

---

[1] If one wants to apply a desired control torque $\tau_d \in \mathbb{R}^3$ at a given time $\bar{t}$, the equation $S(\tilde{b}(\bar{t}))m = \tau_d$ has ∞^1 solutions of the form $m = \frac{S^\top(\tilde{b}(\bar{t}))\tau_d}{\|\tilde{b}(\bar{t})\|^2} + \lambda b(\bar{t})\ \forall \lambda \in \mathbb{R} \iff \tilde{b}^\top(\bar{t})\tau_d = 0$.

[2] Although PBSF laws require angular velocity measurements in addition to magnetometer ones, they can actually be implemented by exploiting the *b-dot* principle to estimate the angular velocity. However, this comes at the expense of a non-null steady-state error as for the classic *b-dot* controllers.

geomagnetic field, as computed from equation (4):

$$\dot{\tilde{b}}(t) = \dot{A}\tilde{b}_0(t) + A\dot{\tilde{b}}_0(t). \quad (6)$$

Indeed, by exploiting the kinematic equation (1), equation (6) can be equivalently written as:

$$\dot{\tilde{b}}(t) = S(\omega)A\tilde{b}_0(t) + A\dot{\tilde{b}}_0(t) = S(\omega)\tilde{b}(t) + A\dot{\tilde{b}}_0(t). \quad (7)$$

By commuting the factors in the cross product appearing at the right-hand side of (7) and recalling that $S^\top(\cdot) = -S(\cdot)$, one gets:

$$\dot{\tilde{b}}(t) = S^\top(\tilde{b}(t))\omega + A\dot{\tilde{b}}_0(t). \quad (8)$$

With the derivative of the measured geomagnetic field ($\dot{\tilde{b}}(t)$, hence the name *b-dot* for magnetic controllers based on this principle) written in this form, it is apparent that the first term is proportional to the body angular velocity of the spacecraft, through a (singular) matrix gain ($S^\top(\tilde{b})$) which is a function of the measured magnetic field itself. Furthermore, the presence of the second term, which is proportional to the rate of variation of the geomagnetic field in the orbital frame (as seen from the body frame) can be interpreted as a limit to the precision of the angular velocity information that $\dot{\tilde{b}}$ can provide. By referring to a simplified model of the geomagnetic field, it can be readily seen that the magnitude of $\dot{\tilde{b}}_0(t)$ is proportional to two times the orbital angular rate $\omega_o \in \mathbb{R}_{>0}$ [26], which has a quite small value for LEO missions. Hence, $\dot{\tilde{b}}$ can be considered a meaningful measure of the spacecraft angular velocity provided that its magnitude is significantly larger than the orbital angular rate. As this is typically the case for the initial condition of a detumbling mode, $\dot{\tilde{b}}$ can be considered a valuable source of velocity feedback to decrease the spacecraft kinetic energy.

Among the different choices for the design of a magnetic detumbling controller directly based on the *b-dot* principle, the simplest one is the proportional control law

$$m = -k\dot{\tilde{b}}(t) =: m_{bdot}(t), \quad (9)$$

where $k \in \mathbb{R}_{>0}$ is a scalar gain. When (8) is substituted in (9) and then in (3), the following control torque is obtained:

$$\tau_m(\omega, t) = -kS(\tilde{b}(t))S^\top(\tilde{b}(t))\omega - kS(\tilde{b}(t))A\dot{\tilde{b}}_0(t). \quad (10)$$

The first term is a proportional angular velocity feedback which provides a desirable source of angular velocity dissipation whenever ω is not parallel to $\tilde{b}(t)$. The "residual" term $-kS(\tilde{b}(t))A\dot{\tilde{b}}_0$ acts as small perturbation on the spacecraft dynamics preventing the actual convergence of ω to zero. Considering the kinetic energy of the spacecraft, *i.e.*,

$$T(\omega) := \frac{1}{2}\omega^\top J\omega, \quad (11)$$

the computation of its time derivative along the trajectories of the closed-loop system obtained by substituting (10) in (2) and neglecting the residual term, gives:

$$\dot{T}(\omega, t) = -k\omega^\top S(\tilde{b}(t))S^\top(\tilde{b}(t))\omega. \quad (12)$$

Because the time-varying gain matrix $kS(\tilde{b}(t))S^\top(\tilde{b}(t))$ is positive semi-definite, $\dot{T}(\omega, t) \leq 0$ and from an engineering perspective it can be claimed that the proportional *b-dot* law can instantaneously decrease the angular velocity from the spacecraft as long as ω is not parallel to $\tilde{b}(t)$. Another popular *b-dot* controller is given by the saturated law

$$m = -m_M\sigma\left(k\dot{b}(t)\right) =: m_{sbdot}(t), \quad (13)$$

where $m_M \in \mathbb{R}_{>0}$ is the maximum deliverable dipole moment and $\sigma(\cdot) : \mathbb{R}^n \mapsto [-1, 1]^n \subset \mathbb{R}^n$ is the unit vector-valued decentralized saturation function, namely, $\mathbb{R}^n \ni u \mapsto \sigma(u) := [\,\mathrm{sat}(u_1), \ldots, \mathrm{sat}(u_n)\,]^\top$ in which $\mathbb{R} \ni x \mapsto \mathrm{sat}(x) = \max(\min(x, 1), -1)$ is the standard unit saturation function. For a large k, the saturated *b-dot* law approaches the behavior of the bang-bang like controller [19]:

$$m = -m_M\mathrm{sgn}\left(\dot{b}(t)\right) =: m_{bbdot}(t), \quad (14)$$

where $\mathrm{sgn}(\cdot)$ is the sign function applied componentwise. The main disadvantage of (14) over the proportional (9) and the saturated (13) controllers is related to the larger power consumption due to the use of the maximum dipole moment at all times and the possible chattering behavior implicit in the use of the (discontinuous) $\mathrm{sgn}(\cdot)$ function.

4.2 Projection-based state feedback designs

The methods that we report in this section address the underactuated nature of magnetic control by combining a time-varying projection operation, based on measurement of the geomagnetic field, and a static state feedback, either dependent on the angular velocity or the angular momentum. Following an averaging-based analysis along the lines of [15], we will show that PBSF controllers can be tuned to achieve exponential convergence (rather than the asymptotic result of [10]) without requiring periodic time-variability of the geomagnetic field [27].

The first step in PBSF designs is the projection operation, which is carried out by introducing in (3) a preliminary input of the form:

$$m = \frac{1}{\|\tilde{b}(t)\|^2} S^\top(\tilde{b}(t))v, \tag{15}$$

where $v \in \mathbb{R}^3$ is a virtual control vector. When substituted in (3), the magnetic torque $\tau_m(t)$ can be compactly rewritten as

$$\tau_m(t) = \Gamma(t)v, \tag{16}$$

where the positive semidefinite matrix-valued function $t \mapsto \Gamma(t) \in \mathbb{R}^{3\times 3}$ is defined as:

$$\Gamma(t) := S(b(t))S^\top(b(t)). \tag{17}$$

By referring to the property $S(x)S^\top(x) = \|x\|^2 I_3 - xx^\top$ for any $x \in \mathbb{R}^3$, one observes that $\Gamma(t) = I_3 - b(t)b(t)^\top$, which is the projection matrix onto the plane perpendicular to b at all time instants. The projection-based action embedded in (15) normalizes the effect of the magnetic field and reduces the control effort by canceling out the useless component of v. In the second step of the PBSF design, the virtual input v is chosen as a static feedback:

$$v = -K\omega := v_{PBSF}(\omega), \tag{18}$$

where $K \in \mathbb{R}^{3\times 3}_{>0}$ is a gain matrix. After combining (15) and (18), the closed-loop is described by (1) and by

$$J\dot{\omega} = S(\omega)J\omega - \Gamma(t)K\omega, \quad t \geq 0. \tag{19}$$

Special selections in the context of PBSF designs are angular velocity [10] or momentum [24] feedback: for the former case, the gain matrix in (18) is set to

$$K = kI_3 =: K_{AV}, \tag{20}$$

while for the latter case it is set to

$$K = kJ =: K_M, \tag{21}$$

where $k \in \mathbb{R}_{>0}$ is a scalar gain. For compactness, in the following we will denote AV-PBSF the projection-based controller obtained by using (20) and M-PBSF the one obtained by using (21). Considering the kinetic energy of the spacecraft defined in (11), the computation of its time derivative along the trajectories of the closed-loop system (19) for $K = K_{AV}$ (20) gives

$$\dot{T}(\omega, t) = -k\omega^\top S(b(t))S^\top(b(t))\omega \leq 0. \tag{22}$$

Similarly to the analysis of the proportional *b-dot* controller in Section 4.1, this is not sufficient to prove that ω converges to zero as $t \to \infty$. In particular, when assuming that function $t \mapsto b_0(t)$ is uniformly continuous, a straightfoward application of Barbalat's Lemma shows that the trajectories converge to $\omega = 0$ or to non-trivial solutions having ω parallel to b [3]. The desirable case $\omega = 0$ can be proven under some assumptions on the time-variability of the geomagnetic field. To this aim, it is not convenient to directly resort to equation (19) since the geomagnetic field is expressed in body frame components and thereby depends on a specific solution to (1),(19). The dependence on $b_0(t)$ can be made explicit by substituting (4)-(5) in (19) and by exploiting the properties $S(Ab) = AS(b_0)A^\top$ and $AA^\top = I_3$ $\forall A \in \mathrm{SO}(3)$ to get:

$$J\dot{\omega} = S(\omega)J\omega - A\Gamma_0(t)A^\top K\omega, \tag{23}$$

where

$$\Gamma_0(t) := S(b_0(t))S^\top(b_0(t)) \tag{24}$$

is the projection matrix $\Gamma(t)$ resolved in the ECI frame.

The main advantage of representing the dynamics as in (23) is that $\Gamma_0(t)$ is an explicit function of the geomagnetic field vector expressed in the inertial frame, *i.e.*, as a pure function of time.

4.3 Averaging-based convergence analysis of PBSF designs

We now exploit the tools of generalized averaging theory [12] to show that there exists a sufficiently small gain k for which the closed-loop trajectories of (23) converge to $\omega = 0$ exponentially fast and without requiring periodicity of the geomagnetic field time-variation. In particular, the average-based analysis of the PBSF controllers is based on the following Assumption.

Assumption 1 *The considered orbit for the spacecraft satisfies the conditions for the applicability of general averaging theory, specifically, the matrix function $t \mapsto \Gamma_0(t)$ defined in equation (24) has average $\bar{\Gamma}_0$,* i.e.*:*

$$\bar{\Gamma}_0 := \lim_{T\to\infty} \frac{1}{T} \int_t^{t+T} \Gamma_0(\tau)d\tau \tag{25}$$

exists and

$$\left\| \bar{\Gamma}_0 - \frac{1}{T} \int_t^{t+T} \Gamma_0(\tau)d\tau \right\| \leq k_{av}\sigma(T), \quad T \in \mathbb{R}_{>0}, \tag{26}$$

$\forall t \in \mathbb{R}_{\geq 0}$, where k_{av} is a positive constant and $\sigma : \mathbb{R}_{\geq 0} \mapsto \mathbb{R}_{\geq 0}$ is a strictly decreasing, continuous, and bounded function, such that $\lim_{T\to\infty} \sigma(T) = 0$.

Remark 1 *As pointed out in [17], Assumption 1 is satisfied by most orbits of practical interest and difficulties*

[3] The same analysis can be easily done for the M-PBSF controller by considering the function $V_M(\omega) := \frac{1}{2}\omega^\top J^2 \omega$.

may arise only for orbits with low inclination with respect to the geomagnetic equator. Note also that the assumption is formulated in terms of so-called generalized averaging, so that the elements of $\Gamma_0(t)$ *are not assumed to be periodic functions of time.*

Theorem 1 *Consider the closed-loop attitude dynamics of the magnetically actuated spacecraft described by (1), (23). Under Assumption 1, if the average matrix* $\bar{\Gamma}_0$ *is positive definite along the spacecraft orbit and the gain matrix* K *is selected as in equation (20) or (21), then there exists* $k^\star > 0$ *such that for any* $0 < k < k^\star$ *the angular velocity* ω *converges exponentially fast to zero for all initial conditions.*

PROOF. We address only the case $K = K_{AVF}$ (equation (20)) since the same steps can be followed for the momentum feedback (21) just by using $\frac{1}{2}z_2^\top J^2 z_2$ as a Lyapunov candidate instead of the one in equation (32).

Consider the closed-loop system (1),(23) and introduce the coordinates transformation

$$Z_1 = A \qquad z_2 = \frac{\omega}{k} \tag{27}$$

in which the system is described by the equations:

$$\dot{z}_1 = kS(z_2)Z_1 \tag{28}$$
$$J\dot{z}_2 = kS(z_2)Jz_2 - kZ_1\Gamma_0(t)Z_1^\top z_2. \tag{29}$$

System (28)-(29) satisfies all the hypotheses for the applicability of general averaging theory [12], which yields the averaged system:

$$\dot{Z}_1 = kS(z_2)Z_1 \tag{30}$$
$$J\dot{z}_2 = kS(z_2)Jz_2 - kZ_1\bar{\Gamma}_0Z_1^\top z_2. \tag{31}$$

As a result, there exists $k^\star > 0$ such that for any $0 < k < k^\star$ the trajectories of system (30)-(31) are close to the trajectories of system (28)-(29).

We now show that all the solutions of (30)-(31) converge to $\omega = 0$ exponentially fast. Consider the $\mathcal{C}^1$ function

$$V_T(z_2) := \frac{1}{2}z_2^\top J z_2 = T(\omega(z_2)), \tag{32}$$

whose time derivative along the flows of (30)-(31) is:

$$\dot{V}_T(Z_1, z_2) = z_2^\top J\dot{z}_2 \tag{33}$$
$$= kz_2^\top S(z_2)Jz_2 - kz_2^\top Z_1\bar{\Gamma}_0Z_1^\top z_2 \tag{34}$$
$$= -kz_2^\top Z_1\bar{\Gamma}_0Z_1^\top z_2 \le -k\lambda_m(\Gamma_0)\|z_2\|^2. \tag{35}$$

where we used $kz_2^\top S(z_2)J_0z_2 = kz_2^\top(J_0z_2 \times z_2) = 0$ thanks to the property of the cross product operator. Therefore, the compact set

$$\left\{(z_1, z_2) \in \mathrm{SO}(3) \times \mathbb{R}^3 : V_T(z_2) \le c,\ c \in \mathbb{R}_{\ge 0}\right\} \tag{36}$$

is positively invariant. As the vector field $F(z_1, z_2) := (kS(z_2)Z_1, kS(z_2)Jz_2 - kZ_1\bar{\Gamma}_0Z_1^\top z_2)$ is smooth, then by [3, see the lemma reported in the proof of Theorem 6.14], the system has a unique solution defined $\forall t \ge t_0 \ge 0$. A straightforward application of Krasovskii-LaSalle invariant set theorem guarantees that all solutions converge to the equilibrium set $\left\{(Z_1, z_2) \in \mathrm{SO}(3) \times \mathbb{R}^3 : z_2 = 0\right\}$.

Furthermore, since $V_T(z_2)$ is quadratic in z_2, namely,

$$\lambda_m(J)\|z_2\|^2 \le V_T(z_2) \le \lambda_M(J)\|z_2\|^2, \tag{37}$$

$\dot{V}_T(Z_1, z_2)$ satisfies the following inequality along the system solutions:

$$\dot{V}_T \le -k\frac{\lambda_m(\bar{\Gamma}_0)}{\lambda_M(J)}V_T. \tag{38}$$

As a result, $V_T(t) \le V_T(t_0)\exp\left(-k\frac{\lambda_m(\bar{\Gamma}_0)}{\lambda_M(J)}(t - t_0)\right)$ $\forall t \ge t_0 \ge 0$ and therefore the convergence of $z_2(t)$ to zero is exponential. By general averaging theory, there exists a sufficiently small k for which all solutions of the original time-varying system converge to $\omega = 0$ exponentially fast as well.

Although the scope of the analysis proposed above seems to be limited by the small gain requirement embedded in Theorem 1, we will show in the next section that using large gains is actually counterproductive.

5 Intrinsic performance limitation of existing PBSF detumbling methods

It has been pointed out in several contributions that selecting the gain k in PBSF or proportional *b-dot* controllers that ensures a fast detumbling is challenging [10,14,24]. Contrary to what one may expect, increasing the gain in (18) does not speed up the convergence to zero of the angular momentum. In this section we formally prove this fact following the reasoning of [10], although we propose an alternative analysis with some new insights. Henceforth we focus on the AV-PBSF controller, although similar conclusions can be drawn for the M-PBSF controller. Essentially, a large gain results in fast dissipation of $\omega_{\perp b} := \Gamma(t)\omega$ (the component of ω orthogonal to b), so that $\omega \to \omega_{\| b} := (b^\top\omega)b$ and the control moment $\tau_m(t) = -k\Gamma(t)\omega$ becomes almost null very quickly because $\Gamma(t)\omega \to \Gamma(t)\omega_{\| b} = 0$. Since there is not much control torque available in this situation, the dissipation of $\omega_{\|b}$ gets extremely slow. To better clarify this point, we inspect the behavior of $\|\omega_{\perp b}\|$ and of $\|\omega_{\|b}\|$ as the gain in (20) increases. In the following derivation, we exploit the fact that $\dot{b} = S(\bar{\omega}(t))b$ for some time-varying (bounded) function $t \mapsto \bar{\omega}(t) \in \mathbb{R}^3$, so that the time derivative of $\Gamma(t)$ can be compactly written as $\dot{\Gamma}(t) = S^\top(\bar{\omega}(t))bb^\top + bb^\top S(\bar{\omega}(t))$. Computing the time derivative of $\|\omega_{\perp b}\|^2$, one gets:

$$\begin{aligned}\frac{\mathrm{d}\|\omega_{\perp b}\|^2}{\mathrm{d}t} &= \frac{\mathrm{d}}{\mathrm{d}t}\omega^\top\Gamma(t)^\top\Gamma(t)\omega = \frac{\mathrm{d}}{\mathrm{d}t}\omega^\top\Gamma(t)\omega \\ &= 2\omega_{\perp b}^\top S^\top(\bar{\omega})\omega + 2\omega^\top\Gamma J^{-1}(S(\omega)J\omega - k\Gamma\omega) \\ &= 2\omega_{\perp b}^\top\left(S^\top(\bar{\omega})\omega + \Gamma J^{-1}(S(\omega)J\omega)\right) - 2k\omega_{\perp b}^\top J^{-1}\omega_{\perp b} \\ &\leq -\tfrac{2(1-\theta)k}{\lambda_M(J)}\|\omega_{\perp b}\|^2 - \|\omega_{\perp b}\|\left(\tfrac{2k\theta}{\lambda_M(J)}\|\omega_{\perp b}\| - r(\omega(t_0))\right)\end{aligned} \tag{39}$$

for $t \geq t_0 \geq 0$, where $\theta \in (0,1)$ and $r(\omega(t_0))$ is a positive scalar function arising from the boundedness of $\omega(t)$ for any initial conditions (thanks to inequality (22)). Note that in deriving (39), we used $\omega = \omega_{\perp b} + \omega_{\|b}$ and $\omega^\top S(x)\omega = 0 \;\forall x \in \mathbb{R}^3$. By means of standard arguments, we can conclude that $\omega(t)$ converges in finite time to the set $\Omega_\perp := \left\{\omega \in \mathbb{R}^3 : \|\omega_{\perp b}\| \leq \frac{r(\omega(t_0))\lambda_M(J)}{2k\theta}\right\}$ and stays therein for all future times. Note that the larger k the smaller is the set $\Omega_\perp$ and the faster is the convergence. Instead, the time derivative of $\|\omega_{\|b}\|^2$ reads:

$$\begin{aligned}\frac{\mathrm{d}\|\omega_{\|b}\|^2}{\mathrm{d}t} &= \frac{\mathrm{d}}{\mathrm{d}t}(\omega^\top b)b^\top b(b^\top\omega) = \frac{\mathrm{d}}{\mathrm{d}t}\omega^\top bb^\top\omega \\ &= -2\omega_{\perp b}^\top S^\top(\bar{\omega})\omega + 2\omega_{\|b}^\top J^{-1}(S(\omega)J\omega - k\Gamma\omega) \\ &= 2\omega_{\perp b}^\top S^\top(\bar{\omega})\omega + 2\omega_{\|b}^\top J^{-1}(S(\omega)J\omega) - 2k\omega_{\|b}^\top J^{-1}\omega_{\perp b}.\end{aligned} \tag{40}$$

One immediately sees that a too fast convergence of $\omega_{\perp b}$ to zero would make $\frac{\mathrm{d}\|\omega_{\|b}\|^2}{\mathrm{d}t} \approx 0$ and would keep the value of $\|\omega_{\|b}\|$ almost constant. It is also worth noting that for an almost spherical spacecraft, the time evolution of $\|\omega_{\|b}\|$ is completely determined by $2\omega_{\perp b}^\top S^\top(\bar{\omega})\omega$: it is not directly affected by the value of k. These results prove that using a large gain induces a motion in which the angular velocity of the spacecraft constantly tracks the direction of $\tilde{b}(t)$ with an almost constant magnitude. The analysis of [10] showed that a "good" value of the gain k to prevent such undesired behavior can be found by equating the order of magnitude of the active and "rotational" terms (those related to $\bar{\omega}(t)$) in the dynamics of $\omega_{\perp b}$). By referring to a circular LEO orbit, the quasi-optimal gain for the AV-PBSF controller proposed in [10] is:

$$k = 2\omega_0(1 + \sin\xi_m)\lambda_m(J) =: k_{opt}, \tag{41}$$

where $\omega_o \in \mathbb{R}_{>0}$ is the orbital angular velocity, ξ_m the orbit inclination relative to the geomagnetic equatorial plane and $\lambda_m(J)$ is the minimum moment of inertia of the spacecraft.

6 A projection-based method for fast magnetic detumbling

In this section we present a novel PBSF controller developed to improve the performance of classic projection-based designs which suffer from the large gain/slow convergence problem described in the previous section. The convergence analysis that we propose is based on Lyapunov theory for time-varying systems: through a suitable selection of the feedback, we show that the closed-loop system is a cascade interconnection and we can conclude global exponential convergence of closed-loop solutions to $\omega = 0$ without any bound on the controller gains.

The control law that we suggest using is a projection-based momentum feedback of the form:

$$m = -k(\omega, \tilde{b}(t))\frac{1}{\|\tilde{b}(t)\|^2}S^\top(\tilde{b}(t))J\omega, \tag{42}$$

in which $(\omega, t) \mapsto k(\omega, \tilde{b}(t)) \in \mathbb{R}_{>0}$ is a gain function. By plugging (42) in the spacecraft dynamics (2)-(3), the closed-loop in body coordinates is given by (1) and by:

$$J\dot{\omega} = S(\omega)J\omega - k(\omega, \tilde{b}(t))\Gamma(t)J\omega. \tag{43}$$

The closed-loop model takes a more useful form for analysis purposes when referred to the inertial frame. Indeed, by considering the angular momentum expressed in the ECI frame, *i.e.*, the change of coordinates

$$h = A^\top J\omega = J_0(A)A^\top\omega, \tag{44}$$

$J_0(A) := A^\top JA$, the closed-loop reads:

$$\dot{A} = AS^\top(J_0^{-1}(A)h) \tag{45}$$

$$\dot{h} = -\tilde{k}(h, A, t)\Gamma_0(t)h \tag{46}$$

where we defined $\tilde{k}(A,h,t) := k(\omega(A,h), A^\top\tilde{b}(t)) = k(\omega(A,h), \tilde{b}_0(t))$. By restricting the class of gain functions to those dependent on (h,t) only, the closed-loop has a cascade structure in which the upper subsystem is described by a time-varying differential equation (46) and perturbs the attitude kinematics (45). Incidentally, the kind of gains that we suggest adopting to improve performance belong to this class. With respect to Section 4, we consider the following Assumption regarding the time-variability of the geomagnetic field.

Assumption 2 *Along the considered orbit for the spacecraft, the geomagnetic field satisfies Assumption 1 and the convergence function $\sigma(\cdot)$ defined in equation* (26) *is* *such that* $\sup_{T\in[0,\infty)}(k_{av}T\sigma(T)) := \bar{\sigma}$*, where* $\bar{\sigma}$ *is a positive scalar.*

Remark 2 *Assumption 2 is only mildly more restrictive than Assumption 1 and it holds,* e.g.*, for a finite power or periodic and almost periodic geomagnetic field [24,12], which cover all the cases of engineering interest [4].*

Let us now introduce the time-varying matrix

$$M(t) := \int_0^t \left(\bar{\Gamma}_0 - \Gamma_0(\tau)\right) d\tau, \tag{47}$$

which will be useful in the proof of Theorem 2. It can be shown that under Assumption 2, $M(\cdot)$ satisfies the inequality:

$$\|M(t)\|_\infty := \sup_{t\in\mathbb{R}_{\geq 0}} \left\| \int_0^t \left(\bar{\Gamma}_0 - \Gamma_0(\tau)\right) d\tau \right\| \leq \bar{\sigma}. \tag{48}$$

Theorem 2 *Consider the dynamical system described by equations* (1)-(3) *and controlled by* (42) *in which* $k(\omega, \tilde{b}(t)) =: k$ *is any scalar function that is locally Lipschitz in* $\omega \in \mathbb{R}^3$*, piecewise-continuous in* t *and such that* $k_m \leq k(\omega, \tilde{b}(t)) \leq k_M$ $\forall(\omega, t) \in \mathbb{R}^3 \times \mathbb{R}_{\geq 0}$ *for some strictly positive scalars* k_m*,* k_M*. If the geomagnetic field satisfies Assumption 2, then the angular velocity* ω *converges exponentially fast to zero for all initial conditions.*

PROOF. To proceed with the proof, we consider the closed-loop represented in inertial coordinates (45)-(46). Let us consider the $\mathcal{C}^1$ function

$$V(h,t) := h^\top \left(\frac{\lambda}{2} I_3 - M(t)\right) h \tag{49}$$

for which it is easily verified that there exist positive constants c_1, c_2 such that

$$c_1\|h\|^2 \leq V(h,t) \leq c_2\|h\|^2, \tag{50}$$

once a sufficiently large λ is selected. Furthermore, it can be shown that the time derivative of $V(h,t)$ along the system dynamics satisfies the following inequality:

$$\dot{V}(h,t) = -\, h^\top Q(t) h \tag{51}$$

where

$$Q(t) := (\lambda\tilde{k} - 1)\Gamma_0(t) - \tilde{k}M(t)\Gamma_0(t) - \tilde{k}\Gamma_0(t)M(t) + \bar{\Gamma}_0. \tag{52}$$

Following [15], we now introduce the time-varying matrix $T(t) := \left[\, b_0(t)\; b_1(t)\; b_2(t) \,\right]$, where $b_1(t)$ and $b_2(t)$ are unit vectors such that they form an orthogonal basis together with the direction of the geomagnetic field $b_0(t)$ at all times, namely, $T(t)T^\top(t) = I_3$ $\forall t \geq 0$. By referring to $T^\top QT$ and thanks to the boundedness of $M(t)$ and the lower and upper bounds on $k(\cdot,\cdot)$, it is possible to show that there exists a sufficiently large λ for which

$$\dot{V}(h,t) \leq -c_3\|h\|^2 \tag{53}$$

for some positive scalar $c_3 \in \mathbb{R}_{>0}$. Based on the claims of [12, Theorem 4.10], one can conclude that all closed-loop solutions converge to $h = 0$ exponentially fast. Clearly, by means of the coordinate transformation (44), the same result holds for (43), *i.e.*, the solutions converge to $\omega = 0$ for all initial conditions.

Remark 3 *For the case of momentum feedback with constant gain, Theorem 2 improves the results of Theorem 1 (there is no need to consider "sufficiently" small gains to conclude global exponential convergence), at the expense of a (mild) additional condition (equation* (48)*) on the geomagnetic field. Nonetheless, it is worth underlying that the estimate of the lower bound of the convergence speed is heavily affected by the value of* λ*. Indeed, it is interesting to note that a large value of the gain* k *requires a large value of* λ *in order to enforce the positive definitiveness condition in* (51)*. In turn, this means that the ratio* c_3/c_2*, which is a lower bound on the rate of convergence of* $\|h(t)\|$*, becomes smaller and smaller for increasing* k*.*

6.1 Robustness analysis

In this section we show that the proposed control law is robust to a sufficiently small uncertainty in the knowledge of the inertia matrix and that the closed-loop solutions are globally uniformly ultimately bounded in the presence of an exogenous (bounded) disturbance torque. In the following, suppose that the inertia matrix is decomposed as the sum a nominal and additive (unknown) term as $J_a := J + \Delta J$, where $\Delta J \in \mathbb{R}^{3\times 3}$ is symmetric and such that J_a is positive definite, and suppose that a bounded disturbance torque $\tau_e(t) \in \mathcal{L}_\infty$ is acting on the system. The corresponding closed-loop dynamics for $h := A^\top J_a \omega$ reads:

$$\dot{h} = -\tilde{k}(h,A,t)\Gamma_0(t)h + \tilde{k}(h,A,t)\Gamma_0(t)A^\top \Delta J A J_0^{-1} h + \tau_e \tag{54}$$

where $\tilde{k}(h,A,t)\Gamma_0 A^\top \Delta J A J_0^{-1} h =: g(h,A,t)$ acts as a state-dependent perturbation on the nominal dynamics.

Corollary 1 *Consider the dynamical system described by equations* (1)-(3) *and controlled by* (42) *in which* $k(\omega, \tilde{b}(t)) =: k$ *is any scalar function that is locally Lipschitz in* $\omega \in \mathbb{R}^3$*, piecewise-continuous in* t *and such that* $k_m \leq k(\omega, \tilde{b}(t)) \leq k_M$ $\forall(\omega, t) \in \mathbb{R}^3 \times \mathbb{R}_{\geq 0}$ *for some strictly positive scalars* k_m*,* k_M*. If the geomagnetic field satisfies Assumption 2, then the angular velocity* ω *converges exponentially fast to zero for all initial conditions* *and for a sufficiently small perturbation $\|\Delta J\|$. Furthermore, the closed-loop solutions are globally uniformly ultimately bounded for any bounded exogenous torque.*

PROOF. The proof of the first claim comes from the robustness property associated with exponential stability. To this end, we start by showing that the time derivative of function $V(h,t)$ defined in (49) along the flow of (54) with $\tau_e \equiv 0$ satisfies:

$$\dot{V} \leq -c_3\|h\|^2 + \left\|\frac{\partial V}{\partial h}\right\| \|g(h,A,t)\|. \quad (55)$$

Note that $\left\|\frac{\partial V}{\partial h}\right\| = \|(\lambda I_3 - 2M(t))h\| \leq c_4\|h\|$ for some scalar $c_4 \in \mathbb{R}_{>0}$ due to the boundedness of $M(t)$. At the same time, the perturbation term $g(h,A,t)$ satisfies $\|g(A,h,t)\| \leq \eta(\|\Delta J\|)\|h\|\ \forall (A,t) \in \mathrm{SO}(3)\times\mathbb{R}_{\geq 0}$ for some class-$\mathcal{K}_\infty$ function $\eta(\cdot)$. Then, it is clear that there exists a sufficiently small $\|\Delta J\|$ which guarantees that $\eta(\|\Delta J\|) < c_3/c_4$. In turn, this means that $\dot{V}(h,t) \leq -(c_3-\eta c_4)\|h\|^2$ where $c_3 - \eta c_4 > 0$. Therefore, global exponential convergence to $h=0$ follows from the arguments of [12, Theorem 4.10]. As for the second claim of the Corollary, we note that $V(h,t)$ is an ISS Lyapunov function [12, Theorem 4.19] for the perturbed system so that its solutions satisfy

$$\|h(t)\| \leq \beta(\|h(t_0)\|, t-t_0) + \gamma\left(\sup_{t\in[t_0,t]}\|\tau_e(t)\|\right) \quad (56)$$

for a class$-\mathcal{KL}$ function $\beta(\cdot,\cdot)$ and a class$-\mathcal{K}$ function $\gamma(\cdot)$. Therefore the solutions are globally uniformly ultimately bounded and the proof is completed.

6.2 Gain selection

We will now show and motivate a possible selection of the gain function $k(\omega,\tilde{b}(t))$ which will be used in the simulation example presented in the next section to show the performance improvement of our design with respect to existing approaches. We propose using the following gain function:

$$k(\omega,\tilde{b}(t)) = \bar{k}_1 \exp\left(-\bar{k}_2\left|\frac{\tilde{b}^\top(t)}{\|\tilde{b}(t)\|}\frac{J\omega}{\|J\omega\|+\varepsilon}\right|\right), \quad (57)$$

where $\bar{k}_1$, $\bar{k}_2$ are strictly positive scalars and $0 < \varepsilon \ll 1$ is a constant introduced to have a well-defined gain $\forall\omega \in \mathbb{R}^3$. By noticing that for small ε the argument of the absolute value in (57) is simply the cosine of the angle α between the geomagnetic field and the angular momentum vectors, one sees that (57) can be compactly written as $k \approx \bar{k}_1\exp(-\bar{k}_2|\cos(\alpha)|)$. Hence, function (57) is such that whenever $\alpha = n\pi$, the gain k attains its minimum value whereas the opposite occurs for $\alpha = \frac{\pi}{2} + n\pi$ for $n \in \mathbb{Z}$. According to this design, a large gain is used when a large torque is available for control purposes, thereby improving the convergence rate. On the other hand, a low but always positive gain is used whenever b and ω are almost aligned so that the natural dynamics dominates until a more favorable condition is reached. As a result, the control law prevents the unwanted effect of keeping ω aligned to b, which would end in a slow dissipation of the kinetic energy as discussed in Section 5. Note that (57) is not the only possible selection and alternative gain functions may be defined as long as they satisfy the basic properties mentioned in Theorem 2. Finally, it is easily seen that $k(\omega(A,h),\tilde{b}(t)) = k(h,\tilde{b}_0(t))$ as mentioned below equation (46).

7 Simulation example

A simulation example is presented, based on mission scenario related to a typical LEO small spacecraft, with the aim of showing the performance improvement of the proposed controller with respect to existing approaches. In particular, we will compare our results with those of the AV-PBSF of [10] (equation (41)), of the M-PBSF, tuned according to a robust analysis [14], and finally of the classical saturated *b-dot* controller (equation (13)). The performance of all algorithms will be evaluated in consistent manner, by means of a Monte Carlo study in which several statistical parameters are computed and then discussed.

The nominal inertia matrix of the considered spacecraft is $J = \mathrm{diag}(1.2763, 1.12436, 0.5662)\ \mathrm{kg}\cdot\mathrm{m}^2$. The geomagnetic field model in the ECI frame is computed according to the 1995 IGRF coefficients. The spacecraft operates along a circular orbit ($i = 66\,\mathrm{deg}$, $e = 0$) with an altitude of 555 km, a corresponding orbital period of $T = 5746$ s and an orbital angular rate given by $\omega_o = 2\pi/T = 0.001093$ rad/s. The nominal initial conditions are $\omega(0) = (0.1678, 0.1688, 0.1676)$ rad/s and $q(0) = (0.6692, 0.0000, 0.7397, -0.0704)$ (we use quaternions to represent the spacecraft attitude in the simulator). It is worth remarking that the initial value of the $\|\omega\|$ is about 50 times larger than the orbital angular rate, which is a fairly conservative initial condition of a detumbling phase. The control laws are implemented in discrete time at 1Hz. To evaluate performance in a plausible environment, actuators saturation is included in the spacecraft model: a maximum magnetic dipole moment $m_M = 2.5\ \mathrm{A}\cdot\mathrm{m}^2$ is assumed for each coil. Furthermore, the effect of environmental disturbances (gravity gradient, residual dipole moment and secular term) are accounted for, specifically, the following disturbance is considered [26]:

$$\tau_e := 3\omega_o^2 S(JA_{rel}e_1)A_{rel}e_1 + S(\tilde{b}(t))m_{res} + A\tau_{\sec}, \quad (58)$$

where $A_{rel} := AA_{orb}^\top$ is the relative attitude between the Local Vertical Local Horizontal (LVLH) orbital frame and the body one, while $m_{res} = \begin{bmatrix} 0.03 & 0.03 & 0.003 \end{bmatrix}^\top$ A $\cdot$ m^2 and $\tau_{\text{sec}} = \begin{bmatrix} 1 & 1 & 1 \end{bmatrix}^\top \cdot 1e^{-7}$N $\cdot$ m is a secular term.

7.1 Controllers tuning

First of all, we present the procedures employed to tune the considered controllers. The unique gain of the saturated *b-dot* controller was tuned by trial and error procedures from which $k = 10^6$ was chosen. Instead, the quasi-optimal gain of the AV-PBSF controller proposed by [10] is $k_{opt} = 0.0024$, as computed from equation (41) with the data of this example. A Monte Carlo study has been carried out to define a robust tuning of the gain k in the M-PBSF controller, with respect to: uncertainty on the initial angular rate ($\pm 50\%$ of an initial reference value chosen as 50 times the orbital angular rate, per axis); uncertainty on the attitude (± 1 on all components of the attitude quaternion); uncertainty on the moments of inertia ($\pm 10\%$ on each of the principal moments). More precisely, 50 simulations were carried out for different choices of the gain k, to assess the settling time of $\|\omega\|$ with respect to a threshold equal to three times the orbital angular rate. The following statistics are computed: mean, standard deviation, maximum and minimum values. Note that the optimal gain k_{opt} is a good candidate to select the range of gains to be considered in the Monte Carlo tuning strategy. The numerical results are depicted in Figure 1, from which $k = 0.004$ is chosen, which guarantees a worst-case settling time of about 0.6 orbits. For what concerns the proposed controller (42) with the gain function (57), a similar tuning procedure has been performed with respect to $\bar{k}_1$, which turned out to be the most influential and difficult parameter to tune, while we selected $\bar{k}_2 = 6$ by trial and error(we fixed $\varepsilon = 0$ without encountering any numerical issue in the simulations). By inspecting the results shown in Figure 2, $\bar{k}_1 = 0.065$ is the gain value that provides the most satisfactory results for the considered orbit, with a worst-case settling time of about 0.5 orbits.

7.2 Monte Carlo simulations

In this section we discuss the results of Monte Carlo simulations (500 runs) carried out with the selected tunings. The same levels of uncertainty described in the previous section have been considered for the simulations. The most relevant statistical parameters (mean, standard deviation, maximum and minimum values) obtained with the different controllers are collected in Table 1 while Figure 3 to Figure 6 depict the corresponding time-domain representations. By analyzing these results, it is clear that the proposed controller outperforms the other designs, with a maximum and average settling time that are reduced up to about $20-30\%$ with respect to the M-PBSF, which is the one providing the best results among the other considered controllers.

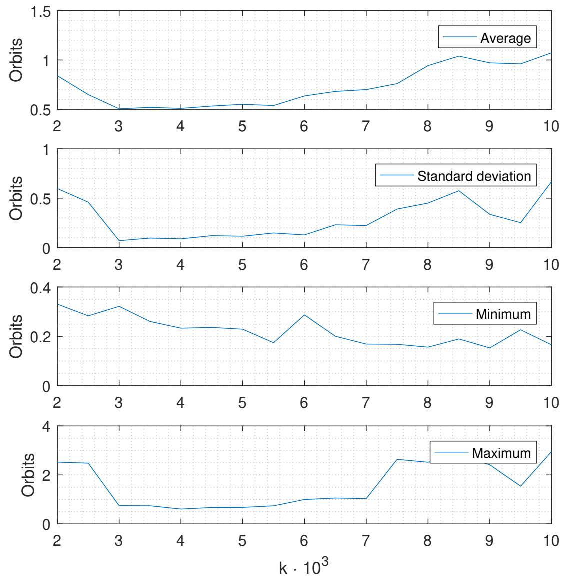

Fig. 1. Monte Carlo tuning statistics - M-PBSF controller.

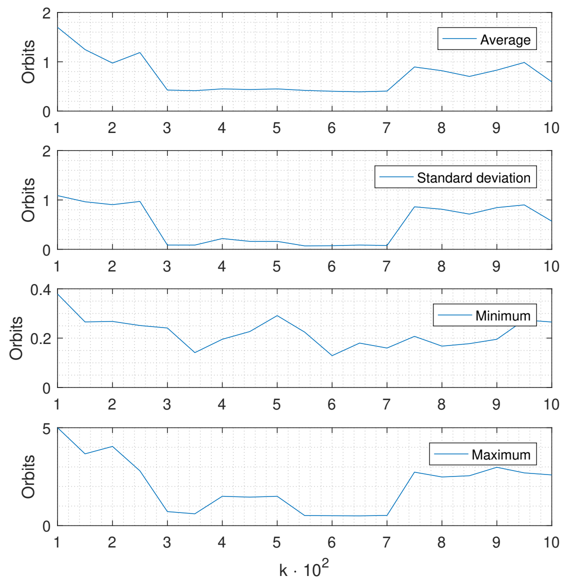

Fig. 2. Monte Carlo - proposed controller (42).

7.3 Performance improvement in the unsaturated regime

In the results presented above, the spacecraft operates most of the time with saturated actuators due to the large magnitude of the nominal initial angular velocity that has been considered. Due to saturation, all the control laws behave in the same way for a significant part of the detumbling maneuver. In case initial conditions are more favorable, the spacecraft operates for

Table 1
Statistical properties comparison [$\%orbit$] - Monte Carlo simulations with 500 runs.

Statistical parameter	Saturated b-dot	AV-PBSF[10]	M-PBSF	Proposed controller
Mean	1.3142	0.6011	0.5216	0.4186
Standard deviation	0.33676	0.0936	0.0844	0.0727
Min	0.4467	0.3100	0.2406	0.1592
Max	2.0936	0.9011	0.6231	0.5257

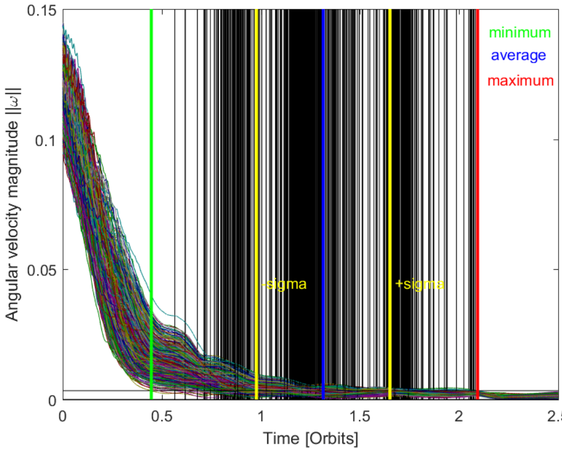

Fig. 3. Monte Carlo simulation - saturated *b-dot* controller (13).

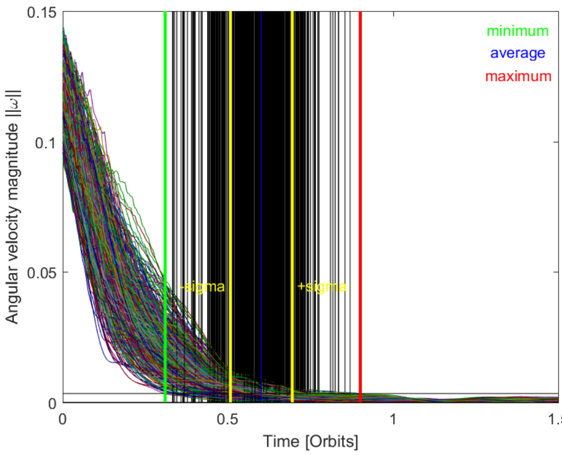

Fig. 4. Monte Carlo simulation - controller proposed in [10].

a larger time in unsaturated conditions and the performance improvement obtained by the proposed controller is actually much sharper. This can be seen by inspecting the results in Table 2, obtained by our controller and by the M-PBSF (the one giving the best results in the previous comparison) in a Monte Carlo study identical to the one of the previous section but considering $\omega(0) = (0.0165, 0.0175, 0.0163)\,\text{rad/s}$, *i.e.*, an initial nominal angular velocity with a magnitude 10 times

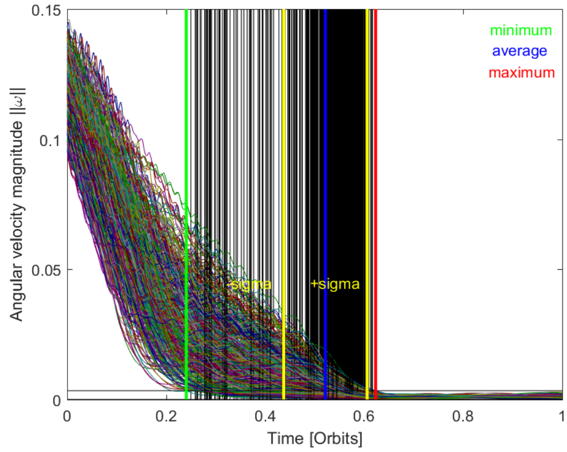

Fig. 5. Monte Carlo simulation - M-PBSF.

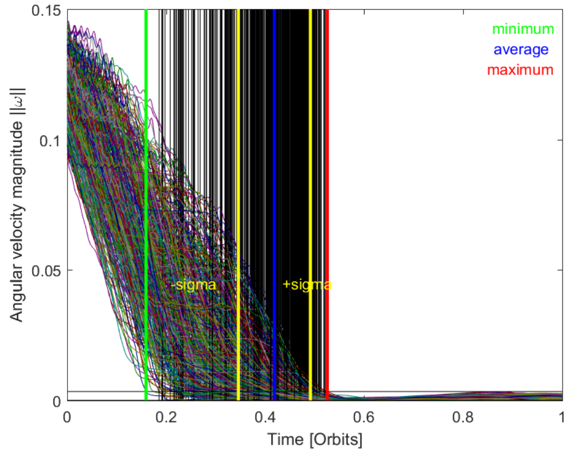

Fig. 6. Monte Carlo simulation - proposed controller (42).

greater than the orbital rate.

8 Concluding remarks

The problem of magnetic detumbling of spacecraft attitude was considered. Novel convergence analyses based on tools from averaging and Lyapunov theory were presented for existing detumbling control methods. We systematically studied the intrinsic performance limitation of projection-based controllers in which selecting

Table 2
Second example - statistical properties comparison [$\%orbit$]

Parameter	M-PBSF	Proposed controller
Mean	0.2381	0.1612
Standard deviation	0.1058	0.0714
Min	0.0749	0.0253
Max	0.4944	0.3912

a large gain leads to a slow convergence rate. To overcome this undesirable behavior, we proposed a novel projection-based momentum feedback controller with a time-varying and state-dependent gain. By taking into account mild assumptions on the time-variability of the geomagnetic field, we were able to prove global exponential convergence of the angular momentum in ideal conditions and for small uncertainties in the knowledge of the inertia matrix. Furthermore, we showed that the closed-loop solutions are globally uniformly ultimately bounded in the presence of (bounded) disturbance torques. By means of a simulation example, it was shown that the novel control law can be tuned to notably improve the transient performance with respect to existing methods. For the considered case, Monte Carlo simulations showed a reduction up to about 30% of the detumbling time as well as a significant reduction of the worst-case settling time.

References

[1] S. Ahmed and E.C. Kerrigan. Suboptimal predictive control for satellite detumbling. *Journal of Guidance, Control and Dynamics*, 37(3):850–859, 2014.

[2] C. Arduini and P. Baiocco. Active magnetic damping attitude control for gravity gradient stabilised spacecraft. *Journal of Guidance and Control*, 20(1):117–122, 1997.

[3] F. Bullo and A. D. Lewis. *Geometric Control of Mechanical Systems: Modeling, Analysis, and Design for Mechanical Control Systems.* Springer, 2005.

[4] F. Celani. Robust three-axis attitude stabilization for inertial pointing spacecraft using magnetorquers. *Acta Astronautica*, 107:87–96, 2015.

[5] C. J. Damaren. Comments on "Fully magnetic attitude control for spacecraft subject to gravity gradient". *Automatica*, 38(12):2189, 2002.

[6] E. L. de Angelis, F. Giulietti, A. H. J. de Ruiter, and G. Avanzini. Spacecraft attitude control using magnetic and mechanical actuation. *Journal of Guidance, Control, and Dynamics*, 38(11):564–573, 2015.

[7] E.J. Findlay, A. De Ruiter, J.R. Forbes, H.H.T. Liu, C.J. Damaren, and J. Lee. Magnetic attitude control of a flexible satellite. *Journal of Guidance, Control and Dynamics*, 36(5):1522–1526, 2014.

[8] T. W. Flatley, W. Morgenstern, A. Reth, and F. Bauer. A b-dot acquisition controller for the RADARSAT spacecraft. In *NASA conference publication*, volume 3345, pages 79–90, 1997.

[9] R. Fonod and E. Gill. Magnetic detumbling of fast-tumbling picosatellites. In *69th International Astronautical Congress, Bremen, Germany*, 2018.

[10] F. Giulietti and G. Avanzini. Magnetic detumbling of a rigid spacecraft. *Journal of Guidance, Control and Dynamics*, 35(4):1326–1334, 2012.

[11] D. Invernizzi and M. Lovera. Attitude stabilization of inertial pointing spacecraft using magnetic actuators. In *21st IFAC Symposium in Automatic Control in Aerospace , Cranfield, UK*, 2019.

[12] H.K. Khalil. *Nonlinear systems.* Prentice Hall, 2001.

[13] M. Lovera. Optimal magnetic momentum control for inertially pointing spacecraft. *European Journal of Control*, 7(1):30–39, 2001.

[14] M. Lovera. Magnetic satellite detumbling: The b-dot algorithm revisited. In *Proc. American Control Conf. (ACC)*, pages 1867–1872, 2015.

[15] M. Lovera and A. Astolfi. Spacecraft attitude control using magnetic actuators. *Automatica*, 40(8):1405–1414, 2004.

[16] M. Lovera and A. Astolfi. Global magnetic attitude control of inertially pointing spacecraft. *Journal of Guidance, Control and Dynamics*, 28(5):1065–1072, 2005.

[17] M. Lovera and A. Astolfi. Global magnetic attitude control of spacecraft in the presence of gravity gradient. *IEEE Transactions on Aerospace and Electronic Systems*, 42(3):796–805, 2006.

[18] M. Lovera, E. De Marchi, and S. Bittanti. Periodic attitude control techniques for small satellites with magnetic actuators. *IEEE Transactions on Control Systems Technology*, 10(1):90–95, 2002.

[19] F. Markley. Attitude control algorithms for the solar maximum mission. In *Guidance and Control Conference*, pages 59–69, 1978.

[20] M. Pittelkau. Optimal periodic control for spacecraft pointing and attitude determination. *Journal of Guidance, Control and Dynamics*, 16(6):1078–1084, 1993.

[21] M. Psiaki. Magnetic torquer attitude control via asymptotic periodic linear quadratic regulation. *Journal of Guidance, Control and Dynamics*, 24(2):386–394, 2001.

[22] E. Silani and M. Lovera. Magnetic spacecraft attitude control: A survey and some new results. *Control Engineering Practice*, 13(3):357–371, 2005.

[23] A.C. Stickler and K.T. Alfriend. An elementary magnetic attitude control system. *Journal of Spacecraft and Rockets*, 13(5):282–287, 1976.

[24] J. Trégouët, D. Arzelier, D. Peaucelle, C. Pittet, and L. Zaccarian. Reaction wheels desaturation using magnetorquers and static input allocation. *IEEE Trans. on Control Systems Technology*, 23(2):525–539, 2015.

[25] P. Wang and Y. Shtessel. Satellite attitude control using only magnetic torquers. In *AIAA Guidance, Navigation, and Control Conference and Exhibit, Boston, USA*, 1998.

[26] J. Wertz. *Spacecraft attitude determination and control.* D. Reidel Publishing Company, 1978.

[27] R. Wisniewski and M. Blanke. Fully magnetic attitude control for spacecraft subject to gravity gradient. *Automatica*, 35(7):1201–1214, 1999.

[28] R. Wisniewski and L.M. Markley. Optimal magnetic attitude control. In *14th IFAC World Congress, Beijing, China*, 1999.

[29] M. Wood, W .H. Chen, and D. Fertin. Model predictive control of Low Earth Orbiting spacecraft with magnetotorquers. In *IEEE International Conference on Control Applications, Munich, Germany*, 2006.

[30] X. Xia, C. Guo, and G. Xie. Investigation on magnetic-based attitude de-tumbling algorithm. *Aerospace Science and Technology*, 84:1106–1115, 2019.